Korean J. Chem. Eng., 40(5), 1037-1044 (2023)
DOI: 10.1007/s11814-022-1323-9

pISSN: 0256-1115
eISSN: 1975-7220

Diffusion behavior of THO, Sr, Cs, and Am through concrete and its chemical degradation

Chung-Kyun Park†, Tae-Jin Park, Jae-Kwang Lee, and Jang-Soon Kwon

Korea Atomic Energy Research Institute, Daedukdaero 989-111, Yousung, Daejon 34057, Korea
(*Received 5 July 2022 • Revised 7 October 2022 • Accepted 23 October 2022*)

Abstract−To understand the transport processes in a repository silo for radioactive waste, the diffusion behavior of tritium (THO), strontium (Sr), cesium (Cs), and americium (Am) through concrete was investigated using a through-diffusion setup. The concrete and groundwater used in this study were sampled from the waste repository site. The diffusivity of the nuclides was obtained by a linear curve fitting of the diffused concentration data against time. After 18 months, the concrete coupons and solutions were recovered from the experimental setups. A sequential chemical extraction was carried out with the recovered coupons to determine the types of sorption involved in the nuclides diffusion processes. The THO transported freely through the concrete pores without sorption. The sorption of Sr and Cs was reversible, whereas that of Am was highly irreversible with a very low diffusivity. After a year in the diffusion test, some precipitate and suspended matter were observed. The precipitates were analyzed with SEM, EDS, and XRD. Identified as calcium carbonates and magnesium compound, they are likely formed by the chemical degradation of the concrete.

Keywords: Diffusion, Sorption, Concrete, Degradation, Sequential Extraction

INTRODUCTION

In the field of radioactive waste management, concrete is widely used as an engineered barrier in radioactive waste repositories and also for solidifying or conditioning matrix of the waste. Korea operates a silo-type repository for low- and intermediate-level radioactive wastes (L&ILW) at a depth of about 80-130 m below ground. When radioactive wastes are disposed in the underground facility, the silo concrete can be the main barrier against the intrusion of groundwater. However, when it comes to long-term management of the wastes, groundwater may slowly penetrate through the concrete and finally contact the waste matrix. Then nuclides in the solid matrix may leach out by the groundwater and confront the silo concrete to move toward biosphere. Diffusion is considered to be the main escaping process for the nuclides in the silo. In the long run, these dissolved nuclides can transport through the geological media and reach to the biosphere. This makes it important to measure the diffusivity of source term nuclides through the concrete matrix, and finally to both understand transport processes around the repository and assess radiological safety of the disposal.

Silo concrete is a mixture of hydrated cement, sands, and crushed rocks. The hydrated cement surrounds the aggregates and other additives by forming a continuous paste matrix. The main chemical components of the anhydrous cement are calcium silicate, calcium aluminate, and calcium aluminate ferrite. When cement contacts water, it forms hydrated continuous solid phases such as calcium silicate hydrate (CSH), calcium hydroxide, and calcium aluminate hydrate (CAH). However, the properties of concrete and porewater can change with time. As a result, the dissolved nuclides can interact with concrete and undergo various kinds of reactions, including sorption at hydrous surfaces, precipitation, lattice incorporation in the cement hydrates, complexation, and the formation of colloids in solution phase.

The porosity of the concrete is one of the most important parameters affecting nuclide transport through it. In normal concrete, the porosity is 10-15% by volume and the pore size ranges from 10^{-9} to 10^{-3} m [1]. The concrete pores consist of gel pores and capillary pores in the hydrated cement paste, pores between the aggregates and aggregate interfaces, and voids due to incomplete consolidation. When concrete is used as a barrier, the mechanical and chemical properties of concrete will change slowly with time. Degradation of the concrete is initiated by an exchange between the initial pore solution and infiltrated groundwater, followed by dissolution of the cement [2,3].

The sorption and diffusion of nuclides into the matrix of the silo concrete can be complex, since it can be affected by changes in environmental conditions such as pH, redox state, and salinity. A fresh cement can generate hyper-alkaline conditions with a pH of up to 13. The pH of the pore solution will also change with the deterioration of the concrete. Gradual changes in the early stage of cement leachate with a pH between 13 and 10 can induce degradation of the hydrated cement [4].

According to Ochs et al. [2], hydrated cement shows four distinct stages of degradation. At the early stage, pore solutions contain high concentrations of free alkali metal ions such as Na^+, K^+, and Ca^{2+} resulting from the initial dissolution of Na_2O, K_2O and $Ca(OH)_2$. Thus, equivalent concentrations of hydroxyl ions are produced and pH is in a range between 12.5 and 13.5. When all alkali

†To whom correspondence should be addressed.
E-mail: ckpark@kaeri.re.kr

ions are removed, the pH of the pore solution will be about 12.5 and controlled by the solubility of portlandite, $Ca(OH)_2$. Druteikiene et al. [5] reported that portlandite was formed in cement after four months of its hydration and was responsible for the alkalinity of the solution in the batch sorption tests. After complete dissolution of the $Ca(OH)_2$, pH will be decreased and regulated by the incongruent dissolution of the CSH phases. Finally, the CSH and other hydrated cement will be completely dissolved and pH will drop to below 10. The composition of the pore solution is governed by the remaining aggregate minerals including calcite and the contacted groundwater.

Many researchers have studied the diffusion and sorption of radionuclides in concretes and cements [6-10], and suggested several immobilization mechanisms for the radionuclides in cement pore water [5,11]. However, most of them carried out the experiments for a relatively short range of time within six months. Thus, they did not give much weight in the degradation of concrete in sorption and diffusion process.

In this work, we determined the diffusivity of representative nuclides through concrete and classified their associated sorption types. We used THO, Sr, Cs, and Am, because they represent non-sorbing, weakly sorbing with a charge of 2+, 1+, and strongly sorbing multi-valent nuclide, respectively. To determine the sorption types in the diffusion processes, we conducted a sequential chemical extraction. The extent of the chemical degradation of the concrete on diffusion more than a year after the test was also investigated.

MATERIALS AND METHODS

The concrete and the groundwater used in this study were sampled from the L&ILW repository site of Korea. The concrete samples were processed as coupons with a thickness and diameter (ϕ) of 0.55 and 5 cm, respectively. The concrete was made by mixing and solidifying cement, sand and crushed rocks together. This means that each concrete sample did not have a homogeneous composition of minerals. Fig. 1 shows the surface of a concrete coupon sample with large particles consisting of biotite, orthoclase, and plagioclase. Small particles of quartz coated with oxidized iron were distributed widely. Some samples which were pierced by pores were discarded. The porosity and density were measured with a water saturation method, and showed mean values of 0.049 and 2.25 g/cm^3, respectively. The water saturation method involves using the volume of the concrete sample and the difference in weight between the dried one and the fully saturated with water [15]. Before the diffusion experiment, the concrete coupons were placed in vacuum to remove the air from the concrete pores, and then placed into a water flask for a month to become saturated with the groundwater. When groundwater was sampled, the properties of the groundwater,

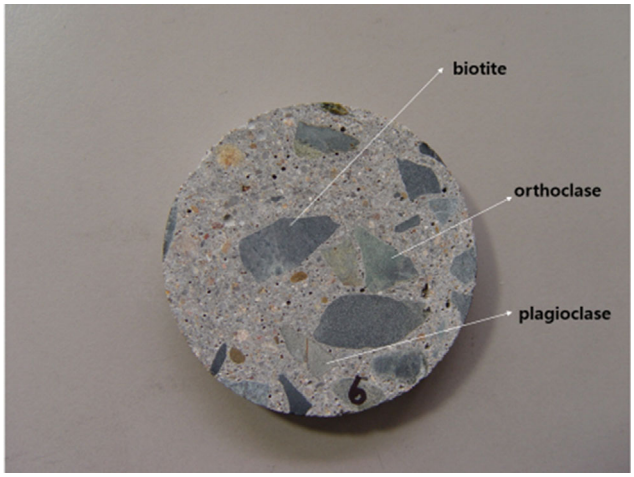

Fig. 1. Slice of concrete coupon used for the diffusion test.

such as pH, Eh, electrical conductivity (EC), and dissolved oxygen (DO), were measured with a multi-parameter meter (Orion Research model 1230) in a flow cell at the repository site. Alkalinity was also measured by titration with a 0.05 M HCl solution at the site. After conditions of the field measurements were stabilized, groundwater was sampled through the flow cell and minimized contacting with the air. The groundwater was filtered through 0.45 μm filter to remove suspended particles. Major cations (Na, K, Mg & Ca) and SiO_2, and minor elements were determined by ICP-AES (Jobin Yvon Ultima 2) and ICP-MS (Elan DRC II), respectively. Anions including Cl and SO_4 were determined by Ion Chromatography (Dionex 1100). The concentration of HCO_3 was calculated from the data of alkalinity and pH. The integrated results showed that dominant cation and anion are alkali metal (Na+K) and HCO_3, respectively. The properties and chemical compositions of the groundwater are arranged in Table 1.

A schematic diagram of the through-diffusion equipment is shown in Fig. 2. The source solution was put into the outer cell, while the groundwater was placed into the inner cell. A concrete coupon was fitted into the bottom of the central cell and the space between the concrete and acrylate wall was sealed with a silicone adhesive.

Four chemical species were used in experiments. Tritium was prepared in the form of tritiated water (THO). Strontium and cesium were prepared as chemical compounds, such as $SrCl_2$ and CsCl. In addition, the radioactive tracer Am-241 was used. A few experimental setups were prepared for each species using different concrete samples to check the effects of heterogeneity of the concrete samples.

The diffusion experiment was initiated by placing the tracer-con-

Table 1. Properties and chemical composition of the groundwater

Aqueous property	pH		Eh (mV)		EC (μS/cm)			DO (mg/l)		Ionic Strength (IS)				
	7.3		103		151			4.6		0.39				
Element mg/l	Na	K	Mg	Ca	SiO_2	Cl	SO_4	HCO_3	Fe	Sr	Mn	Li	B	Ba
	17.7	1.8	4.4	10.4	53.7	15.7	18.4	39.7	2.1	0.1	0.26	0.01	0.02	0.09

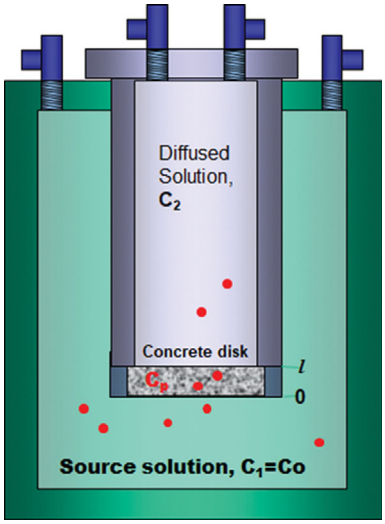

Fig. 2. Schematic diagram of the through-diffusion experimental setup.

taining solution into the source cell, after a blank solution of groundwater had been placed in both cells for a month. The concentrations of the source solutions were about 385 mg/l of Sr, 538 mg/l of Cs, 195 bq/ml of THO, and 591 bq/ml of Am-241, which was equivalent to about 2×10^{-8} mol/l. The diffusion sets were shaken mildly by mechanical motion. At an appropriate time interval, 1 ml aliquots were taken from both cylinder cells to check change of the concentration. Equivalent volumes of the solutions were added to maintain the balance between the two cells and to keep the concentration of the source constant.

After the diffusion experiment, the equipment was dismantled and the concrete coupons were recovered. Chemical extraction was carried out on the recovered concrete coupons to determine the types and amounts of nuclides sorbed during the diffusion as following steps [14,16].

Each recovered concrete coupon was put in 200 ml of tracer-free groundwater in a batch container to achieve back-diffusion and desorption. After a week, all of the concrete samples were recovered for the next step. Secondly, the samples were put into 200 ml of a tracer-free 0.5 M $CaCl_2$ solution for a week. Thirdly, KCl, Fourthly, a mixture of 0.175 M ammonium oxalate ($(NH_4)_2C_2O_4$) and 0.1 M oxalic acid ($H_2C_2O_4$) at pH 3. Fifthly, a solution mixture (SSC) of 3.33% sodium dithionite ($Na_2S_2O_4$) in 0.15 M sodium citrate ($C_6H_5Na_3O_7$) and 0.05 M citric acid ($C_6H_8O_7$) buffer. And finally, aqua regia.

For the each extraction step, the batch containers were put into an oven and kept about 50 °C to accelerate the extraction reactions. The tracer concentration in the solutions was measured at each extraction step. Parallel to the diffusion test, a batch sorption test was carried out for a month with crushed concrete powder in the groundwater to grasp sorption property of the concrete separately. The radioactivity of the tritium and Am-241 was measured using a Packard liquid scintillation counter and the concentrations of Sr and Cs were analyzed using a Varian ICP-MS (inductively coupled plasma - mass spectrometry).

DIFFUSIVE TRANSPORT MODEL

When diffusing through concrete pores, nuclides can also sorb on the surface of the concrete pore walls. If we consider that sorbed nuclides are transported by surface diffusion, then the overall or apparent diffusion effects can be described by the two diffusion mechanisms of pore and surface diffusion. Then the rate of concentration change in the concrete pore can be described as Eq. (1) [12].

$$\varepsilon\frac{\partial C_p}{\partial t}+(1-\varepsilon)\rho\frac{\partial q}{\partial t}=\varepsilon\frac{\delta}{\tau^2}D_v\frac{\partial^2 C_p}{\partial x^2}+(1-\varepsilon)\rho D_s\frac{\partial^2 q}{\partial x^2} \quad (1)$$

where C_p is the concentration in a concrete pore, q is the sorbed concentration on the concrete's surface, D_v is the diffusivity in water, D_s is the surface diffusivity, ε and ρ are the porosity and density of the concrete, respectively.

The initial and boundary conditions of a through-diffusion system, as shown in Fig. 2, can be described as

$C_1(t=0)=Co$ (constant)
$C_2(t=0)=0$
$C_p(x, 0)=0$ $0\le x<l$
$C_p(0, t)=C_o$ $t\ge0$
$C_p(l, t)=C_2(t)$ $t\ge0$

where C_o is the initial concentration in the source cell, $C_1(t)$ and $C_2(t)$ are the concentration in the source cell and diffused cell at time t, respectively, and l is the thickness of the concrete coupon.

The detailed process for getting the solution could be found in the references [13,16], and the analytical solution was given as Eq. (2).

$$\frac{C_2(t)}{C_o}=\frac{D_aR}{lh}t-\frac{lR}{6h} \quad (2)$$

where D_a is the apparent diffusivity, h is the cylinder length of the diffusion cell in Fig. 2, R is the capacity factor, $R=\varepsilon+(1-\varepsilon)\rho K_d$, and K_d is the distribution coefficient of a species between solid and aqueous phase.

The apparent diffusivity, D_a, is defined as Eq. (3).

$$D_a=\frac{\varepsilon D_p+(1-\varepsilon)\rho K_d D_s}{\varepsilon+(1-\varepsilon)\rho K_d} \quad (3)$$

where D_p is the pore diffusivity.

From the slope of the linear curve fitting of $C_2(t)/C_o$ as a function of time (t) using Eq. (2), the apparent diffusivity, D_a, can be determined. For nonsorbing species, D_a becomes D_p as K_d approaches to zero in Eq. (3). Thus, Eq. (2) can be modified for a nonsorbing tracer as Eq. (4).

$$\frac{C_2(t)}{C_0}=\frac{D_e}{lh}t-\frac{l\varepsilon}{6h} \quad (4)$$

where D_e is the effective diffusivity.

RESULTS AND DISCUSSION

The diffusion concentrations for the four nuclides were normalized as a function of time in Fig. 3. We ran two different concrete

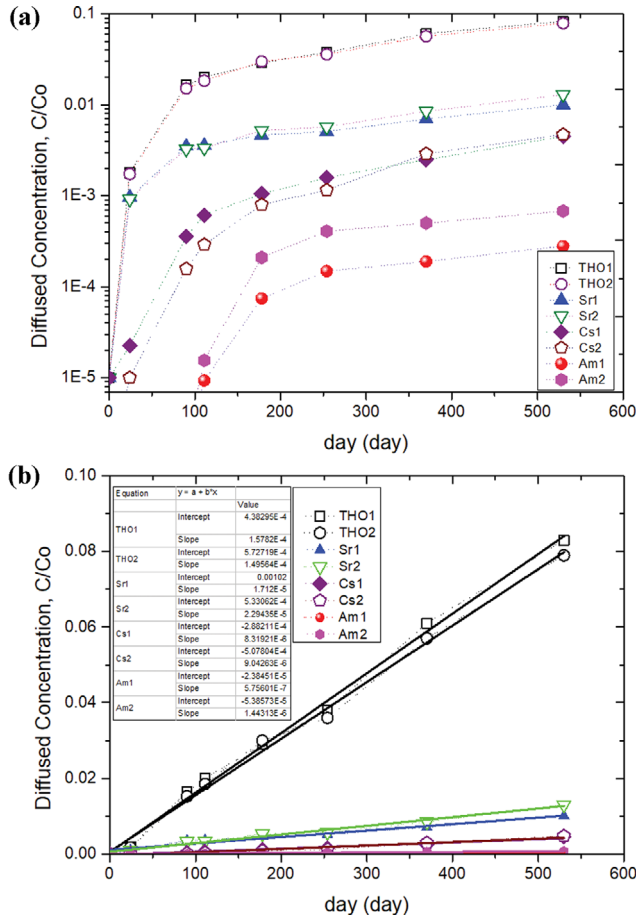

Fig. 3. Diffusion curves of the nuclides as a function of time (a) and their linear curve fits to get diffusivity (b).

samples for each nuclide, designated species 1 and species 2 in Fig. 3. Their curves do not show significant differences between the pair of the nuclides. This suggests that the inhomogeneity of the mineral composition of the concrete samples did not have a noticeable effect on the diffusion process.

For tritium, as the non-sorbing tracer, the normalized diffused concentration (C/C_0) was reached about 0.1 after 1.5 years of diffusion, as shown in Fig. 3(a). For Am, as the highly sorbing tracer, C/C_0 was around 0.001. That is, only 0.1% of Am diffused out through the concrete after 18 months at the concentration level. The values of D_e for THO or D_a for the sorbing tracers were determined from the slopes of the linear curve fitting using Eq. (2) or (4), as shown in Fig. 3(b). The D_v values of the tracers were taken from the literature [15]. The diffusivities of the nuclides obtained for the concrete are summarized in Table 2.

To evaluate the geometric hindrance of the pore structures of the concrete on the diffusion process, the relationship between diffusivities was applied: $D_e=D_p\ \varepsilon=D_v\ \varepsilon\delta/\tau^2$. The calculated mean value of D_e for tritium was 9.5×10^{-13} m^2/s, and the porosity (ε) was 0.049, which is relatively small compared to the 0.1-0.15 of normal concrete as mentioned in the introduction section. The reason could be the high hydration of the cement and a large portion of the aggregates. Then the geometric factor (δ/τ^2) was calculated to be 0.0081, which is very small value compared to that of a crystalline rock of 0.096 with a porosity of 0.0027 obtained under the same experimental conditions [16]. This signifies that even though the porosity of the concrete was much larger than that of the crystalline rock, the geometric factor of the concrete was much lower than that of the rock. It could be due to not only geometric hindrance, but also electrochemical hindrance, the high alkalinity in the pores of the concrete. As mentioned in the introduction section, there were many Na^+, K^+ ions in the pores of the concrete, and those ions may prevent tracers from penetrating by acting as an electrochemical barrier to diffusion. The D_a or D_p values of THO were fairly comparable with to the other concrete data given in Table 2 [7,8,10]. Further comparison was not possible due to limited access to basic data such as porosity and geometric factor in the other tests.

For the sorbing cations, Sr, Cs and Am, the D_a values were arranged in the "measured" column in Table 2. Generally, slopes of the diffusion curves of nuclides were roughly in inversely propor-

Table 2. Diffusivities of the nuclides into the concrete (unit : m^2/s)

Nuclide	K_d (ml/g)	D_v ($\times10^{-9}$)	D_p ($\times10^{-11}$)	D_e ($\times10^{-13}$)	D_a			
					Concrete			Granodiorite
					D_e/R	Measured	Reference data	[16]
THO	0	2.4	1.98 1.88	9.7 9.2 0.8-33 [7] 60 [10]	1.94×10^{-11}	1.98×10^{-11} 1.88×10^{-11}	1.8×10^{-11} [8] $0.5\text{-}2\times10^{-11}$ [7] 3.7×10^{-11} [10]	23×10^{-11}
Sr	60	0.68	0.55	2.7 0.3-4.1 [7]	20×10^{-16}	7.78×10^{-16} 10.0×10^{-16}	$2.3\text{-}6.5\times10^{-13}$ [7] $0.9\text{-}4\times10^{-16}$ [18]	54×10^{-16}
Cs	54 1-10 [9]	2.4	1.94	9.5 13-18.6 [7]	78×10^{-16}	4.2×10^{-16} 4.6×10^{-16}	$3\text{-}3.5\times10^{-13}$ [7] $2\text{-}7.7\times10^{-14}$ [9] $0.3\text{-}2\times10^{-16}$ [18]	4.7×10^{-16}
Am	1857 10^3-10^4 [9]	1.0	0.8	3.97	95×10^{-18}	0.85×10^{-18} 2.12×10^{-18}	$3\text{-}8\times10^{-18}$ [9]	17×10^{-18}

tion to their K_d values. If there is a certain discrepancy in such trend, we could consider another possibility on sorption and diffusion process, for example, sorption reversibility or surface diffusion. To express the retardation effects for a sorbing tracer by a geometric hindrance and sorption, the apparent diffusivity, D_a, can be modified as follows.

$$D_a = \frac{\varepsilon D_p + (1-\varepsilon)\rho K_d D_s}{R} \cong \frac{D_e}{R} + D_s \quad (5)$$

In Eq. (5) the first term of the numerator expresses the retardation effects of a geometric hindrance, and the second term expresses the sorbed phase diffusion. When surface diffusion is the dominant process, the obtained D_a is expected to depend on the sorption properties of the nuclide. When there is no surface diffusion, D_a can be determined solely by the first term, D_e/R, in Eq. (5), and thus the values of D_e/R were calculated and given in the "D_e/R" column in Table 2. The calculated D_e/R values of all the sorbing nuclides were somewhat greater than the measured D_a values. This implies that there was no considerable surface diffusion for these sorbing nuclides, and K_d (or R) was smaller than that from the batch sorption test, probably due to the difference of the media state between powder in the batch and coupon in the diffusion test.

The obtained D_e values of Sr and Cs were similar to Atkinson et al's data [7]. Regarding the D_a values, Plecas et al. [18] obtained similar or slightly lower values, while others have reported much larger values [6,7,9]. These results could be partially due to differences in the sorption ability of the concretes. For Cs, Allard et al. [19] obtained K_d values about 1 to 10 ml/g with ten types of concretes, while in this experiment, K_d was 54, about five times higher than Allard's. The D_a values of Sr and Cs are decreased in the order of 10^5 compared to that of THO mainly due to their sorption on the concrete.

For Am, the measured D_a and K_d values matched Albinson et al's results [9]. The strong sorption tendency of Am resulted in a small D_a value of 10^{-18} m^2/s. Ochs et al. [2] noted that sorption of Am on cementitious materials is mainly due to surface complexation, followed by fixation into CSH structures, and thus it becomes irreversible. It is well known that Am sorbs more on biotite than other minerals in the aggregates of concretes [19]. In this experiment the concrete specimens contained a certain amount of biotite and other rock minerals, as shown in Fig. 1.

At the initial stage of the diffusion test, the solubility limit of Am in the source solution at pH 7.3 is above 10^{-6} mol/l [2], while the initial concentration of Am in this experiment was about 10^{-8} mol/l. As time passes, some Am complexes may be formed $Am_2(CO_3)_3$ or Am-CO_3-OH due to carbonate ions in the groundwater or degradation of the concrete. These complexes can prevent diffusion through the pores of the concrete, even though it produces only minor effects [21]. In post-experiment such Am compounds were not identified among the separated precipitates and suspensions. The dominant oxidation state of Am is trivalent under aerated aquatic systems. Thus, Am^{3+} ion and a tri-carbonate complex species, $Am(CO_3)_3^{-3}$, are presumed to be dominant in groundwater of Eh=103 mV in this system, and can diffuse into the pores of the concrete. On the other hand, the concentration of dissolved carbonate is very low in the concrete pores due to the strong alkaline condition in the pores. When a sorption test was carried out with the same concrete but powered in a batch, the final pH of the solution was about 12.4 after one month. Thus, we can guess the pH in the pores was over 12.4. Under such pH condition, Am has a strong tendency of hydrolysis to form $Am(OH)_3$ and also an equilibrated type, $Am(OH)_3$(s), which has a very low solubility limit of 5×10^{-10} mol/l. Moreover, Am sorbs strongly on the concrete. Thus, owing to the low solubility limit in the strong alkaline condition and the high sorption on the concrete, the diffusivity of Am could be very low compared to that of Sr and Cs. The final diffused concentration of Am was in the level of 10^{-11} mol/l in the inner diffusion column.

To quantitatively determine the diffusion and sorption mechanisms of the sorbing nuclides onto concrete, sorption reversibility was evaluated based on the sequential chemical extraction. Table 3 and Fig. 4 show the extraction results of the nuclides sorbed onto the concrete coupons. As shown in Fig. 1, the concrete matrix is composed of not just cement, but also several kinds of rocks and mineral phases. Thus, sorbing nuclides may interact with those materials in various ways. The fraction desorbed by the groundwater includes loosely sorbed species retained in the concrete by relatively weak electrostatic attraction. Sr and Cs showed a certain amount of reversible sorption, and Cs displayed a more desorbed portion than Sr. Sr also showed a higher K_d value than Cs. This trend between Sr and Cs on the concrete is the opposite of that observed for rocks and soils.

When the sorbed species are extracted by $CaCl_2$, a readily exchangeable fraction can be released by the displacing action of Ca^{+2}, which is an ion-exchange reaction. This was also the case for Sr and Cs in this experiment. Sr had the largest portion, indicat-

Table 3. Percentage of sorption types of the nuclides on concrete (unit: %)

Nuclide	Sorption type	Reversible	Weak IX	Strong IX	am.Fe	cr.Fe	Fixed
	Extractant	GW	$CaCl_2$	KCl	am.oxalate	SSC	Aqua regia
Sr		14	32	11	1.5	25	16
Cs1		30	6	47	7	10	1.7
Cs2		30	38	19	5	1	7
Am1		0	0.1	0.1	2.7	85	12
Am2		0.7	0.7	1.8	11	59	27

* IX: ion exchange, am.Fe: amorphous iron oxide, cr.Fe: crystalline iron oxide
SSC: mixture of sodium dithionite and sodium citrate

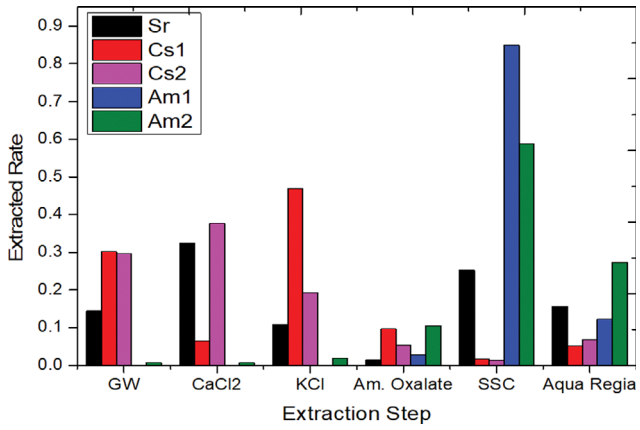

Fig. 4. Sequential results for the extraction of nuclides from concrete.

ing that the exchange with Ca was the main sorption mechanism for Sr.

Extraction with KCl also replaces the sorbed nuclides via ion-exchange. K^+ also acts as a stronger exchanger than Ca^{+2} and penetrates more deeply into the mineral inner structure. This is particularly effective for Cs, because K^+ has a similar size and charge to Cs^+, and hence they show similar sorption characteristics and can access the interlayer of the mineral structure. Consequently, Cs showed more distinct portion in the KCl extraction than Sr and Am.

Fractions that are strongly bound by covalent forces, typically on the hydrous oxides of manganese and iron (Fe-Mn), are increasingly less mobile over time. Ammonium oxalate dissolves amorphous iron oxide (am.Fe) and releases the bound nuclides by the reductive dissolution of this sediment fraction. The more crystalline fraction requires a stronger reducing agent for dissolution. The SSC solution was used with the aim of recovering the nuclides associated with the more crystalline iron oxide fraction (cr.Fe). The association with Fe-Mn oxides was the main sorption mechanism of Am in the concrete, as shown in Table 3 and Fig. 4, which indicates that Am must be sorbed irreversibly mainly on the aggregates, especially on the biotite, as explained in the previous section.

One more interesting result is that about 25% of the Sr was extracted by the SSC solution. This implies that Sr binds more strongly on the aggregates and penetrates deeply into the matrix. On the while, in geologic media like rocks and soils, Sr is usually reacted by ion exchange, and it has been reported that about 90% of sorbed Sr can be extracted by $CaCl_2$ and KCl [16]. Such difference between media in sorption of Sr could be caused by the high alkalinity of the concrete pore and will be discussed later.

Even after the concrete specimens were treated with the five kinds of extracting reagents described above, there were still some nuclides remaining in the concrete. They were presumed to be firmly fixed in the mineral structure. In such cases, most of the nuclides were still likely bound to the concrete structure, had penetrated deeply into the concrete structure, and were irreversibly sorbed. This is called fixation or mineralization. The specimens were finally digested in the aqua regia. Am displayed the strongest fixation, and Sr also showed about 16% fixation.

The reversibility of the sorption can give a hint on mobility related to migration and diffusion of a nuclide. A reversibly sorbing species binds loosely onto the surface of the concrete pores and rebounds again in the solution or moves to an adjacent surface, while an irreversible one hardly does so. In this study, about 57% and 85% of the Sr and Cs were sorbed by the ion exchange mechanism, respectively. On the other hand, Am showed a great irreversible sorption tendency. Irreversibly sorbed nuclides are hard to move on the sorbed phase. Thus, the reversibility of the sorption seems to be one of the key factors controlling diffusion and migration ability. The concept of distribution coefficient, K_d, is based on the assumption of reversible sorption. Therefore, highly irreversible nuclides like Am could be less mobile than expected based on model simulations with K_d in the safety assessment.

From the chemical extraction results, the most distinguishable observation was the strong binding of Sr on concrete. Divalent cations with a radius smaller than Ca^{2+}, such as Ni^{2+}, Co^{2+} or Mg^{2+}, can replace Ca^{2+} [4]. Ca^{2+} exchange by Sr^{2+} might occur in the interlayers of the CSH phases. Sr^{2+} binding to CSH is due to the ion exchange reaction with Ca^{2+} on the edge and planar silanol groups of the CSH phases. Thus, the substitution of Sr for Ca in the cement hydrates is the main sorption mechanism.

At the same time, the portion of strongly bonded Sr was greater than that of Cs. Fig. 4 shows that Cs was sorbed mainly by ion exchange, while Sr showed a certain portion of strong and irreversible bond. Atkinson et al. [6] also obtained similar results from a batch sorption test. It is commonly known that Sr sorbs mainly by weak electrostatic bonding and is located on the outer Helmholtz layer, while Cs can penetrate more deeply into the interlayers of minerals, and consequently exhibits much stronger bonding on geologic media. However, in the strong alkaline condition, the surface of the concrete could be deprotonated by OH^- and charged strongly negative. Then Sr can locate in the inner Helmholtz layer with strong bonding [20-22]. That is, even though divalent Sr^{2+} is dominant under most pH conditions, in hyper-alkaline conditions Sr forms the monovalent $SrOH^+$ species in solution and can build inner sphere complexes like monovalent species, K^+ or Cs^+ [22]. The transition to inner sphere complexes with increasing pH indicates that Sr would sorb more strongly at high pH.

Hietanen et al. [23] found that Cs was preferentially sorbed onto the aggregate in the concrete system, not onto the cement phase, using an auto-radiographic examination. That may be attributed to the high Ca concentration in the solution and the positively charged surface of the silanol groups of CSH, resulting in limited Cs sorption. Noshita et al. [24] reported that Cs did not sorb on calcite. Jakubick et al. [4] also showed that no significant sorption of Cs occurred on cement and carbonate aggregates, but a greater sorption on gneiss aggregates containing mafic minerals such as biotite and pyroxene was found using auto-radiographic analysis. Those studies explain the reason why Cs showed less sorption than Sr in the concrete.

As shown in Table 3 and Fig. 4, the percentage of sorption types differed a little between a couple of species. This is probably due to differences in the mineral composition of the two sets. However, the measured diffusivities of each nuclide pair were consistent in general.

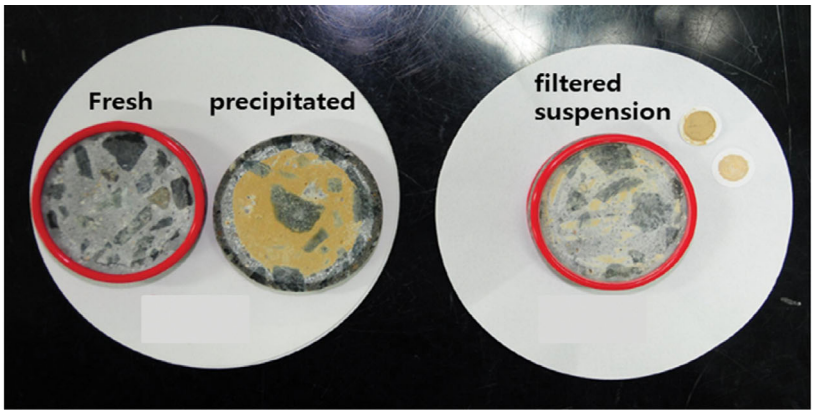

(a)

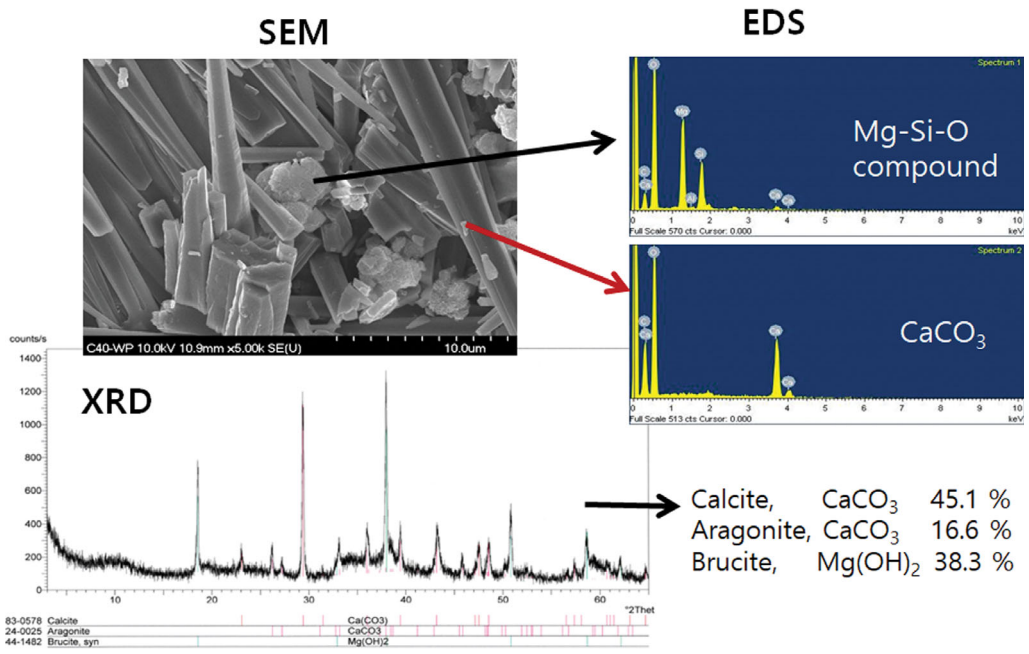

(b)

Fig. 5. (a) Brownish precipitates (left) and filtered suspended matter (right). (b) SEM, EDS, and XRD analyses of the filtered materials.

After a year of diffusion time, brownish precipitates and suspended matter were observed in most of the test setups. When the diffusion test was finished, the precipitates were collected and the suspensions were also filtered, as shown in Fig. 5(a). They were analyzed by scanning electron microscope (SEM) and energy dispersive spectroscopy (EDS), and the results are displayed in Fig. 5(b). The brownish particles turned out to mainly be Mg-Si-O compound. The suspensions were identified as stick-shaped $CaCO_3$ particles with a size of several hundred micrometers. Additionally, the dried suspended matter was analyzed with x-ray diffraction (XRD) to identify their crystalline forms. As a result, two kinds of calcium carbonates ($CaCO_3$), calcite (45.1%) and aragonite (16.6%), were observed. Also brucite ($Mg(OH)_2$) (38.3%), a kind of magnesium hydroxide, was also identified.

The groundwater contained Mg and SiO_2, at concentrations of 4.4 and 53.7 mg/l, respectively, as shown in Table 1. A typical Portland cement roughly contains about 63, 23, and 6% calcium oxide, silica, and alumina, respectively. Some CaO and silica constituents were apparently dissolved from the concrete during the experimental time of more than a year. In this case, there could be a plenty of sources and time to form calcium carbonates and magnesium compounds under the diffusion test conditions. When cement contacts groundwater, calcium hydroxide can be formed; it then reacts with carbon dioxide in the groundwater, and finally calcium carbonate can emerge, as shown in the following reactions:

$$2(3CaO{\cdot}SiO_2)+6H_2O \rightarrow 3CaO{\cdot}2SiO_2{\cdot}3H_2O+3Ca(OH)_2$$
$$Ca(OH)_2+CO_2 \rightarrow CaCO_{3(s)}+H_2O$$

The precipitation of $CaCO_3$ on a concrete surface in contact with groundwater was expected by Allard et al. [19]. As mentioned in the introduction, after one year of testing, the concrete sample seemed to be remarkably degraded considering the appearance of calcite precipitate in the system. Because excessive neoformations can interact with nuclides, it may have an additional sorption effect. How-

ever, there were no notable signals of Sr, Cs, or Am detected in the precipitates, likely due to the very low concentrations of them.

Calcite has a smaller reactive surface area than other sorbing cement materials. That is, it will have lower sorption potential than other cement phases [2]. The literature says that Cs sorbs little on calcite, while Sr and Am sorb better on it [2,24]. Therefore, when the diffusivity of a nuclide through concrete is measured over a relatively long-term scale, the chemical degradation of the concrete should be carefully considered. In accordance with the above description, it is recommended to base estimates of diffusivity on results obtained from a longer experimental time, or with a fully degraded concrete, for the purpose of long-term disposal management.

CONCLUSIONS

The diffusion and related sorption properties of tritium, Sr, Cs, and Am in concrete were investigated and compared with those for other concretes and rocks. The obtained apparent diffusivities of tritium, Sr, Cs and Am were about 2×10^{-11}, 9×10^{-16}, 4.4×10^{-16}, and 1.5×10^{-18} m^2/s, respectively. The diffusivities were about ten times lower than those obtained for granodiorite under the same conditions. Although the obtained level of porosity favors larger diffusivity in concrete than rocks, the strong alkalinity generated in the concrete pores could prevent the diffusion of nuclides in concrete. From sequential chemical extraction, the effects of sorption characteristics on the diffusion of nuclides were identified. When the nuclides pass through the concrete pores, Sr and Cs are sorbed mainly via ion exchange, whereas Am sorbs by fixation to iron oxides or other mineral aggregates. That is the reason why Am shows a very low diffusivity than the other nuclides. Some precipitates and suspensions were observed after a year. It is likely the chemical degradation of concrete resulted in the precipitation, and the precipitates turned out to be calcium carbonate and magnesium compounds.

ACKNOWLEDGEMENTS

This work was supported by the Institute for Korea Spent Nuclear Fuel (iKSNF) and National Research Foundation of Korea (NRF) grant funded by the Korea government (Ministry of Science and ICT, MSIT) (2021M2E1A1085202).

NOMENCLATURE

C_p : concentration in a concrete pore [kg/m^3]
C_o : initial concentration in the source cell [kg/m^3]
$C_1(t)$: concentration in the source cell at time t [kg/m^3]
$C_2(t)$: concentration in the diffused cell at time t [kg/m^3]
D_a : apparent diffusivity [m^2/s]
D_e : effective diffusivity, $D_e=\varepsilon D_p$ [m^2/s]
D_p : pore diffusivity, $D_p=\delta/\tau^2 D_v$ [m^2/s]
D_v : diffusivity in free water [m^2/s]
D_s : surface diffusivity [m^2/s]
h : cylinder length of the diffusion cell [m]
K_d : distribution coefficient of a species between solid and aqueous phase, $K_d=q/C_p$ [m^3/kg]
l : thickness of the concrete coupon [m]
q : sorbed concentration on the concrete's surface [kg/kg]
R : capacity factor of concrete, $R=\varepsilon+(1-\varepsilon)\rho K_d$ [dim'less]
t : elapsed time [s]

Greek Letters

ε : porosity of the concrete [dim'less]
δ : constrictivity [dim'less]
ρ : density of the concrete [kg/m^3]
τ^2 : tortuosity [dim'less]

REFERENCES

1. B. Johannesson, *Transport and sorption phenomena in concrete and other porous media*, Doctoral thesis, Lund Univ. Report TVBM-1019 (2000).
2. M. Ochs, D. Mallants and L. Wang, *Radionuclide and metal sorption on cement and concrete*, Springer (2016).
3. J. Perko, D. Jacques, D. Mallants and L. Wang, ICEM2009-16220 (2009).
4. A. Jakubick, R. Gillham, I. Kahl and M. Robin, *MRS Online Proceedings Library*, **84**, 355 (1986).
5. R. Druteikiene, J. Sapolaite, Z. Ezerinskis and L. Juodis, *J. Radioanal. Nucl. Chem.*, **313**, 299 (2017).
6. A. Atkinson and A. Nickerson, *Nucl. Tech.*, **81**, 100 (1988).
7. A. Atkinson, P. Claisse, A. Harris and A. Nickerson, *Mat. Res. Soc. Symp. Proc.*, **176**, 741 (1990).
8. Z. Szanto, E. Svingor, M. Molnar and Z. Szucs, *J. Radioanal. Nucl. Chem.*, **252**, 133 (2002).
9. Y. Albinson, K. Anderson, S. Borjesson and B. Allard, *J. Cont. Hydrol.*, **21**, 189 (1996).
10. K. Uusheimo, A. Muurinen, J. Lehikoinen and M. Olin, YJT-93-26 (1993).
11. N. Evans, *Cem. Concr. Res.*, **38**, 543 (2008).
12. K. Skagius and I. Neretnieks, *Water Res. Res.*, **24**(1), 75 (1988).
13. J. Crank, *Mathematics of diffusion*, Oxford Univ. Press, New York (1956).
14. D. I. Kaplan and S. M. Serkiz, *J. Radioanal. Nucl. Chem.*, **248**(3), 529 (2001).
15. Y. Ohlsson and I. Neretnieks, SKB TR 97-20 (1997).
16. C. K. Park, M. H. Baik and Y. K. Koh, *Nucl. Tech.*, **196**, 121 (2016).
17. K. Andersson, B. Torstenfelt and B. Allard, SKB-KBS-TR-83-13 (1983).
18. I. Plecas, J. Drljaca, A. Peric, A. Kostadinovic and S. Glodic, *Radio. Waste Man. Nucl. Fuel Cycle*, **14**, 195 (1990).
19. B. Allard, L. Eliasson, S. Hoglund and K. Andersson, SKB-KBS-TR-84-15 (1984).
20. A. Fuller, S. Shaw, C. Peacock, D. Trivedi and I. Burke, *Langmuir*, **32**, 2937 (2016).
21. S. Wallace, S. Shaw, K. Morris, J. Small and I. Burke, *Environ. Sci. Technol.*, **47**, 3694 (2013).
22. B. Collins, D. Sheerman and K. Ragnarsdottir, *Radiochim. Acta*, **81**, 201 (1998).
23. R. Hietanen, E. Kaemaeraeinen and M. Alaluusua, YJT-84-04 (1984).
24. K. Noshita, T. Nishi, T. Yoshida, H. Fujihara, N. Saito and S. Tanaka, *MRS Proceedings*, **663**, 115 (2001).